Default mode and frontal executive network interactions enable interoceptive attention & mindfulness

Gillian Grennan
University of California, San Diego
Pragathi Balasubramani
University of California, San Diego
Vojislav Maric
University of California, San Diego
Dhakshin Ramanathan
University of California, San Diego
Jyoti Mishra (jymishra@ucsd.edu)
University of California, San Diego https://orcid.org/0000-0001-6612-4557

Article

Keywords: breath awareness, mindfulness, EEG, default mode, precuneus, prefrontal cortex, depression

Posted Date: October 4th, 2021

DOI: https://doi.org/10.21203/rs.3.rs-951928/v1

Abstract

Interoceptive attention to internal sensory signals is fundamental to mindfulness. In an attention-to-breathing task in 161 adults, we found that consistency of interoceptive attention significantly correlated with performance efficiency across several exteroceptive cognitive domain tasks. EEG source mapping within subjects showed that on low-consistency or distracted trials there was greater recruitment of frontal executive control activity in the dorsolateral prefrontal cortex (DLPFC) and suppression of the posterior default mode network (Precuneus), with increased functional connectivity between these regions. In contrast, high-consistency or attentive trials were associated with greater connectivity between Anterior Cingulate Cortex (ACC) and Insula, key nodes of the cognitive control network for attention monitoring. Notably, individual trait mindfulness was correlated with greater functional connectivity between DLPFC-Precuneus on distracted trials and greater ACC-Insula connectivity on attentive trials. These results showcase dynamic network interactions underlying objective markers of interoceptive attention and subjective rating mindfulness.

Introduction

Attention is the fundamental basis of cognitive control, enabling selective processing and action on goal-relevant stimuli while suppressing irrelevant distractions[1–3]. Attention can be directed to external stimuli, or internally-generated sensations. Exteroceptive attention is well studied and known to be associated with activity of several top-down control networks, including the fronto-parietal attention network associated with selective processing of sensory features; the salience/cingulo-opercular network, involving the anterior cingulate cortex (ACC) and insula, associated with attentional monitoring; and the dorsal executive network, involving the dorsolateral prefrontal cortex (DLPFC) that is dynamically deployed for moment-to-moment attentional control and distractor suppression[4,5]. Further, activity within the default mode network (DMN) has been linked to subjective mind-wandering reports and is suggested to drive variability in goal-directed behavior on demanding exteroceptive attention tasks[6–8].

Interoceptive attention involves attention to internal sensations generated from the body while learning to monitor and disengage from irrelevant distractions[9,10]. Interoceptive attention is a core skill that can be developed through mindfulness training. Many mindfulness traditions use attention to breath as a base practice to develop interoceptive attention. Studies have shown that breath-focused mindfulness training can improve depression and anxiety and help individuals achieve greater wellbeing[11–13]. Skill in breath counting has also been shown to be an indicator for mindful awareness and better mood[14]. Yet, it has been difficult to study the neural processes underlying attentional lapses/distractions that occur during interoceptive tasks because, during meditation, distractions are not easily identifiable even by the subject, let alone the researcher. Prior attempts to capture neural correlates of interoceptive attention/distraction have used designs contrasting meditation with other tasks (i.e. to capture a “state” effect), or have used random probes or other forms of self-report to retrospectively and subjectively identify distracted vs.

attentive states during meditation[15–20]. Together, these studies have suggested that attentive breath meditation involves regulation/suppression of default-mode brain areas and engagement of executive circuits (including the dorsal prefrontal and salience/cingulo-opercular networks) similar to those observed for exteroceptive tasks[16,21–23]. Breath focused meditation training is also associated with plasticity of anterior cingulate and insula, bolstering this particular network in meditative practice[24,25]. Yet overall, there has been no way to link neural processes to objective measures of interoceptive breath-oriented attention and internal distraction. Thus, the specific role that the DMN, salience/cingulo-opercular and executive control networks play in interoceptive attention performance and distractibility has been difficult to clarify.

In this study, we engaged healthy adults in an interoceptive, attention to breath task. The task involves consistent monitoring of breathing with a motor response (finger-tap) after every two complete cycles of inhalation and exhalation. In contrast to prior studies which rely on subjective reports of distraction, here we used natural variability in the motor responses as a direct, objective marker of interoceptive attentional fluctuations. Greater consistency between responses was used as a marker of improved interoceptive attentional control across subjects. The same approach, within each subject was used to group breath monitoring “trials” as more consistent (attentive) vs. less consistent (distracted). This allowed us to identify neural activity associated with attentive vs distracted trials. We had two goals in this study. First, we aimed to measure whether consistency of interoceptive attention relates to performance on any externally-oriented cognitive tasks. This question is important because it informs how interoceptive attention may link to general cognitive abilities[26], and further validates our approach of using consistency as a relevant marker of interoceptive performance. Second, we aimed to investigate the neural basis of consistent performance within individuals by contrasting attentive vs. distracted epochs of high vs. low consistency, respectively. If interoceptive attention recruits similar cognitive control networks as exteroceptive attention monitoring tasks[4,5], then we hypothesized that we will also observe greater activity or connectivity within core nodes of the salience/cingulo-opercular network during the attentive task trials. By contrast, we hypothesized that on distracted trials, we may find greater activation of DLPFC as a marker for cognitive effort involved in distractor suppression.

Results And Discussion

Interoceptive attention performance is independent of participant demographics and mental health behaviors. 161 healthy adult participants with no history of neuropsychiatric illness and no active meditation experience in the past year as per published criteria[27] consented to the single-visit study. Participants engaged in a simple, eyes-closed attention to breathing task where they were instructed to monitor two breaths at a time, i.e. two complete inhalations and exhalations, and reported completion using a finger-tap motor response. The task was 5 minutes in duration with median ± median absolute deviation (mad) response time of 7.49 ± 2.26 sec across all subjects (Fig. 1A).

Table 1 shows participants demographics of age, gender, race and socio-economic score (SES), the latter assessed using the family affluence scale[28–30]. We also evaluated relevant anxiety, depression, and mindfulness traits using standard self-report measures that have been shown to have high validity and reliability[31–33].

We calculated consistency of interoceptive attention on this task for each subject based on the median response time normalized median absolute deviation across trials (i.e. consistency = 1 – (mad RT/ median RT)). We then ran a robust, multiple linear regression model for consistency on the interoceptive attention task with all demographic and mental health trait factors as predictors, but did not find any significant independent predictors (p>0.2).

Consistency of interoceptive performance correlates with efficiency of exteroceptive cognitive tasks. To probe whether consistency of interoceptive attention is a meaningful marker of cognition, we investigated the correlation of this measure with performance on exteroceptive cognitive tasks that participants performed in the same session. All participants completed a standard set of cognitive tasks for inhibitory control (Go/NoGo task), interference processing (Flanker task), working memory (visuo-spatial delayed match to probe task), and an emotion bias task during the same experimental session as the interoceptive task[29,30]. The task design for each of these assessments is shown in Supplementary Figure 1. We extracted the signal detection sensitivity metric, d-prime, and processing speed as the log inverse of the response time in each task and then combined these two measures in the efficiency metric for each task as the product of d-prime and speed[30,34–36]. Global cognitive efficiency was then calculated as the average performance efficiency across the four cognitive task domains of inhibitory control, interference processing, working memory and emotion bias.

We found that consistency of interoceptive attention was significantly correlated to global cognitive efficiency averaged across all exteroceptive tasks (= 0.133 0.034, p = 0.0001, robust regression plot shown in Fig. 1B). In addition, consistency was significantly correlated to efficiency in each of the cognitive domains tested (inhibitory control: 0.32 0.074, p < 0.0001; interference processing: 0.13 0.040, p = 0.002; working memory: 0.10 0.043, p = 0.016; emotion bias: 0.11 0.040, p = 0.003). These results show that greater consistency of interoceptive attention is directly related to greater efficiency in several cognitive domains, the strongest associations emerging with inhibitory control performance.

Contrasting activations in posterior default mode and frontal cognitive control regions underlie interoceptive attention. All participants underwent electroencephalography (EEG) recordings simultaneous with the interoceptive attention task. We found that 8-12 Hz alpha band oscillations were the dominant frequency of neural oscillations in the eyes-closed attention-to-breath task across all EEG

electrodes (Fig. 2A); alpha dominance during eyes-close rest is well known and our results confirm this neural phenomenon occurs during eyes-closed interoceptive attention as well[37].

Our specific objectives for the neural analysis was to understand the processes supporting consistent interoceptive attention versus those that are engaged when subjects are distracted. For this, we epoched trials based on the finger-tap response made after every two breathing cycles. We separated trials that had high consistency (within 1 mad of median response time) for each subject from those that were slower than expected and of low consistency (greater than 1 mad of median response time). We then contrasted alpha-band source-localized neural activity on high versus low consistency trials using t-tests, with family-wise error rate (fwer) corrections applied for comparisons across the 68 cortical regions of interest (ROIs) that were parcellated as per the Desikan-Killiany atlas during source localization[38]. We focused our analysis on the epoch that preceded each breath monitoring response by ~ one breath cycle [-3.7 to 0] sec, where 3.7 sec is half of the two breath cycle average response time across subjects. This epoch of time represented, on high consistency trials, patterns of neural activity that occur when subjects are on task and attentive, and on low consistency trials, patterns of neural activity that occur when subjects are distracted but then reorient to the task. Importantly, on low consistency trials, by time-locking data to the response, we are most clearly capturing neural processes associated with reorientation to the task and not the “distracted state” per se. Across all participants there were 15.23 5.32 high consistency trials (50.99 1.06% of total trials) and 14.70 5.32 low consistency trials (49.01 1.06% of total trials). 1.74 3.82 trials (5.23 9.25% of total trials) were impulsive trials, i.e. much faster than 1 mad response time and were excluded from further analyses due to potential motor artifact contamination from the prior responses in the relevant [-3.7 to 0] sec epoch window.

Fwer-corrected alpha band results contrasting high and low consistency performance trials are shown in Fig. 2B. We found that core cognitive control regions, including the left DLPFC, insula and ACC, all showed greater activity prior to the response on low consistency trials, when subjects are distracted and in the process of reorienting to the task. These activations may, thus, represent the greater effort to suppress the distraction and reorient to the breath monitoring task. Interestingly, the precuneus, a core region of the posterior DMN, showed significantly lower alpha activity prior to the response on low consistency trials, aligned with the need for DMN suppression during distractor suppression. These specific contrasting activations in the core cognitive control network regions are shown in Fig. 2C, for the bilateral Precuneus (t-stat 6.34 ± 0.001, $p<0.0001$), left DLPFC (t-stat -5.51 ± 0.0001, $p < 0.0001$), left insula (t-stat -3.80 ± 0.001, $p = 0.0002$) and bilateral ACC (t-stat -6.81± 0.0008, $p < 0.0001$). The estimation plots (i.e., paired Gardner-Altman plots) for these data are shown in Supplementary Figure 2. The left lateralization for DLPFC and insula are concordant with our prior work and that of others showing left laterization linked with positive affect and self-regulation[25,29,30,39–41]. Overall, these results show that stable interoceptive attention can be associated with higher levels of DMN Precuneus activity, akin to what has been observed on exteroceptive continuous performance tasks[42–44]. In other words, when subjects are on-task and attentive, DMN Precuneus suppression is not required and may not thus always be the source of non-productive mind wandering[6–8]. However, during the low consistency trials

that have longer response times and are therefore linked with increased distractedness, we find that top-down control regions (DLPFC, ACC, Insula) are more active and DMN Precuneus suppression occurs, potentially reflecting the effort required to suppress distractors and reorient attention back to the interoceptive task. Thus, for the first time, to the best of our knowledge, we show within-task within-subject flexible neural activations that directly underlie interoceptive performance.

We next wanted to study whether the results obtained here are specific to the alpha band or also apply to theta (3-7 Hz) and beta (13-30 Hz) frequency bands. For this we applied the same analytics as above to contrast high and low consistency trials within the theta and beta bands; these contrasts were significantly correlated to the neural contrasts we found in the alpha band (theta vs. alpha band correlations in 68 ROIs, r=0.43 +/- 0.04; t-stat = 10.29 p<0.0001; beta vs. alpha band correlations in 68 ROIs r= 0.53 +/- 0.04; t-stat = 12.08 p<0.0001). Thus, our results for eyes-closed attention to breathing were alpha dominant but not exclusive to the alpha frequency range.

Functional connections between default mode and frontal cognitive control regions flexibly support interoceptive attention. We next investigated functional connectivity between the relevant DMN and cognitive control regions of the bilateral Precuneus, left DLPFC, left Insula, and bilateral ACC for the pre-response breath monitoring epoch. For this, spectral amplitude correlations were conducted on the [-3.7 to 0] sec epoched alpha band data from the relevant ROIs, separately for high consistency and low consistency trials. Functional connectivity contrasts between high and low consistency trials were compared using t-tests with fwer-correction applied for multiple comparisons.

We hypothesized that cognitive control regions may need to be recruited to suppress DMN regions during less consistent interoceptive performance. Aligned with this hypothesis, we observed significantly greater functional connectivity between the Precuneus and left DLPFC prior to response on low consistency trials compared to high consistency trials (Fig. 2D: t-stat = -4.01 ± 0.18, p < 0.0001). We similarly observed greater functional connectivity between the Precuneus and left Insula on low vs. high consistency trials (Fig. 2D: t-stat = -9.72 ± 0.23, p < 0.0001). In contrast to this, on high consistency trials (compared to low consistency trials), we observed greater ACC - Insula functional connectivity (Fig. 2D: t-stat = 3.69 ± 0.30, p = 0.0003). The estimation plots (i.e., paired Gardner-Altman plots) for these data are shown in Supplementary Figure 3. Thus, we found that greater connectivity within the salience/cingulo-opercular network, which has been shown to represent sustained attention, self-regulation and emotional regulation in many studies[5,29,45–47], was associated with improved interoceptive attention on this task. Strikingly, interoceptively oriented meditative trainings that we and others have implemented, have also shown stronger ACC-Insula connectivity post-training, strongly supporting our electrophysiological results[24,48,49].

Functional connections between default mode and frontal cognitive control regions during interoceptive attention predict mindfulness. We performed multiple linear regression analyses to investigate the

relationship between trait mindfulness and alpha band neural activations in core network regions as well as alpha band functional connectivity in these regions. Specifically, to interpret the results presented in the sections above, we wanted to understand how neural activity/functional connectivity differences between high vs. low consistency trials within subjects may potentially serve as markers for subjective mindfulness reported across subjects. The neural activity and functional connectivity models were fwer-corrected for comparisons across these two types of neural features. Additionally, since mindfulness was inversely correlated to anxiety (Spearman's rho = -0.52, p<0.001) and depression (rho = -0.56, p<0.001), these symptoms were accounted for as covariates in the regression models.

The neural activity model included the alpha power difference between high vs. low consistency trials in Precuneus, DLPFC, Insula and ACC as the independent variables. The overall model was significant (R = 0.58, F(6,149) = 12.75, p<0.001). However, no specific neural activity variable was significant in this model (p>.07); depression was the only significant predictor (standardized ß = -0.38, t = -3.75, p<0.001).

The functional connectivity model included the alpha band connectivity difference between high vs. low performance trials for the Precuneus-DLPFC, Precuneus-Insula and ACC-Insula connections that we observed above to be sensitive to change based on trial type. The overall model was significant (R = 0.61, F(5,121) = 14.17, p<0.001). Significant negative predictors of mindfulness in this model included anxiety (standardized ß = -0.22, t = -1.97, p = 0.05), depression (ß = -0.36, t = -3.30, p = 0.001), and Precuneus-DLPFC connectivity (ß = -0.27, t = -2.58, p = 0.01). Interestingly, ACC-Insula connectivity was a positive predictor for mindfulness (ß = 0.28, t = 2.68, p = 0.008). Precuneus-Insula connectivity was a nonsignificant predictor (p>0.4). The partial regression plots for the significant predictors in this model are shown in Fig. 3.

Thus, we found that mindfulness was predicted by flexible connectivity between Precuneus-DLPFC that showed greater connectivity on low vs. high consistency trials, as well as ACC-Insula that showed greater connectivity on high vs. low consistency trials). These results reveal how cognitive control networks within core brain regions in the DLPFC, ACC, Insula and the DMN Precuneus flexibly interact in distinct ways to support the mindfulness trait, a functional measure of real-world behaviors.

Overall, our results show how the core DMN region of the Precuneus and the frontal cognitive control regions of the DLPFC, ACC and Insula modulate and interact to flexibly support interoceptive attention. As has been evidenced for exteroceptive continuous performance tasks[42–44], we find that greater DMN activity in the Precuneus is observed on high consistency i.e. high performance trials of the interoceptive attention to breathing task; however when subjects are engaged in distractor suppression on low consistency trials, DMN activity in Precuneus is likewise suppressed. In contrast, cognitive control regions of the DLPFC, ACC and Insula are upregulated during low consistency trials; this potentially reflects greater cognitive effort required to perform the interoceptive task when subjects are distracted and/or neural processes associated with re-orienting to the task. Functional connectivity results additionally show greater Precuneus – DLPFC connectivity as well as greater Precuneus – Insula activity on low consistency trials, supporting a role for top-down cognitive control activity in suppression of distractions.

Finally, within-network connectivity of the cinguloopercular/salience network was observed to be greater during high interoceptive performance, consistent with a role of these brain regions in self-awareness and self-regulation[5,29,45–47]. Furthermore, our prior research shows that ACC - Insula connectivity is strengthened when interoceptive attention abilities are trained via breath focused meditation[24]. Finally, while mindfulness has been shown to be correlated to attention to breathing, specifically breath counting[14], its functional neural predictors have not been investigated in the context of interoceptive attention. Here, we replicate well known inverse relationships between mindfulness and anxiety/depression. Further, we show that flexible functional connections between Precuneus – DLPFC and ACC – Insula on high versus low performance epochs, can predict trait mindfulness. Thus, for the first time to the best of our knowledge, our results link objective functional neural markers underlying interoceptive attention to subjective mindfulness. These functional markers can be useful neuroplasticity targets in future studies that aim to train interoceptive abilities and mindfulness. A persuasive rationale for training interoceptive abilities such as via breath focused meditation is further driven by our results, which show that consistency of interoceptive attention correlates with efficiency of global multi-domain cognition. In summary, our results show that interoceptive performance ability could be a key determinant of global cognition and we demonstrate the flexible cognitive control and DMN network dynamics that underlie this ability.

Declarations

Acknowledgements

This work was supported by University of California San Diego (UCSD) lab start-up funds (JM), and in part, by seed grants from the T. Denny Sanford Institute for Empathy and Compassion (JM, PB, VM) We thank Fahad Alim, Mariam Zafar-Khan and several UCSD undergraduate students who assisted with data collection. The *BrainE* software is copyrighted for commercial use (Regents of the University of California Copyright #SD2018-816) and free for research and educational purposes.

Author Contributions

G.G. and V.M. conducted the experiments; G.G., P.B. and J.M. analyzed the data; D.R. and J.M. designed the experiments; J.M. wrote the paper and G.G., P.B., V.M., D.R. edited the paper.

Declaration of Interests

The authors declare no conflicts of interest.

Tables

Demographics		median ± mad
Age		22.0 ± 5.45
Sex n (%)		
	Male	65 (40.37)
	Female	96 (59.63)
Race n (%)		
	Caucasian	63 (39.13)
	Black/African American	2 (1.24)
	Asian	48 (29.81)
	Native American	3 (1.86)
	Other	45 (27.95)
SES		5.0 ± 1.61
Mental Health		median ± mad
Anxiety (GAD7)		5.0 ± 3.71
Depression (PHQ9)		4.0 ± 4.21
Mindfulness (MAAS)		4.07 ± 0.75

Table 1. Median and median absolute deviation (mad) scores of the demographic and mental health factors self-reported by study subjects; mental health scales used are shown in parentheses (n=161).

Methods

Participants: 161 healthy adult human subjects, 18-60 years of age participated in the study. All participants provided written informed consent for the study protocol (#180140) approved by the University of California San Diego institutional review board (UCSD IRB).

Demographics and Mental Health. All participants provided demographic information via self-report. This included age, gender, race and ethnicity, socio-economic status (SES) shown in Table 1. Race was reported as 1 of 7 categories (Caucasian; Black/African American; Native Hawaiian/ Other Pacific Islander; Asian; American Indian / Alaska Native; More than one race; Unknown or not reported). SES composite scores were assessed using the family affluence scale: this scale measures individual wealth based on ownership of objects of value (i.e. car/computer) and produces a composite score ranging from 0 (low affluence) to 9 (high affluence) measured on the Family Affluence Scale[28]. No participant had any current/past history of clinical diagnoses or medications. Participants were also meditation-naïve with no active experience in the past year[27].

All participants reported subjective mental health using valid and reliable standard self-report scales for anxiety (7-item Generalized Anxiety Disorder scale GAD-7[50]), depression (9-item Patient Health

Questionnaire PHQ-9[32]) and mindfulness (14-item Mindful Attention Awareness Scale MAAS[33,51]), shown in Table 1.

Neuro-Cognitive Assessments. All assessments, including the interoceptive attention assessment were delivered on the *BrainE* Unity-based platform developed and deployed by NEAT Labs [30,52]. Apart from the interoceptive attention assessment, we evaluated performance on an inhibitory control task, interference processing task, working memory task and emotion bias task (see Supplementary Figure 1 for task designs). The Lab Streaming Layer (LSL[53]) protocol was used to time-stamp each stimulus/response event in each cognitive task. All study participants engaged with the neuro-cognitive assessments on a Windows-10 laptop sitting at a comfortable viewing distance. All assessments were completed within a 40 min session.

1. Interoceptive Attention to Breathing. Participants accessed a task named *Two Tap*. They were instructed to close their eyes and breathe naturally and to respond every two breaths using the laptop spacebar. The computer screen appeared dark gray for the duration of the task, which was 5-minutes, implemented in two 2.5 minute blocks.

2. Inhibitory Control. Participants accessed a game-like task named *Go Wait*. The basic task framework was modeled after the standard test of variables of attention[54,55]. In this two-block task, visual stimuli of colored rockets appeared in either the upper or lower central visual field. The task sequence consisted of a central fixation "+" cue for 500 ms, followed by a rocket stimulus of either blue target color or other iso-luminant non target color, presented for 100 ms. For blue rocket targets, participants were instructed to press the spacebar on the laptop keyboard as quickly as possible ("go" trials). For non-target color rockets (iso-luminant brown, mauve, pink, purple, teal), the participant was instructed to withhold their response until the fixation "+" cue flashed briefly on the screen, at 2 sec for 100 ms duration ("wait" trials). Response feedback was provided for accuracy as a smiley or sad face emoticon presented 200 ms post-response for 200 ms duration, followed by a 500 ms inter-trial interval (ITI). Both task blocks lasted 5 minutes and consisted of 90 trials per block with 30/60 target/nontarget ratio in block 1 and 60/30 ratio in block 2; stimuli were presented in a shuffled order. Four practice trials preceded the first task block, and participants received percent block accuracy score at the end of each block with a series of happy face emoticons (up to 10). All other assessments described below also used the same trial and block summary feedback specifications as in this task to promote task engagement. 82 of 161 participants completed this task as it was introduced later in the data collection process.

3. Interference Processing. Participants accessed a game-like task named *Middle Fish*, which was an adaptation of the Flanker assessment[56–58]. Participants attended to a central fixation "+"cue for 500 ms, and then viewed an array of fish presented either in the upper or lower central visual field for 100 ms. On each trial, participants had a 1 sec response window to detect the direction of the middle fish in the set (left or right) while ignoring the flanking distractor fish that were either congruent or incongruent to the middle fish, i.e., faced the same or opposite direction to the middle fish. 50% of task trials had congruent

distractors and 50% were incongruent. A brief practice of 4-trials preceded the main task of 96 trials presented over two blocks for a total task time of 8 min.

4. Working Memory. Participants accessed a game-like task named *Lost Star*, which was based on the visuo-spatial Sternberg task[59]. The task sequence had the participants attend to a central fixation "+"cue for 500 ms, followed by a spatially distributed test array of objects (i.e., a set of blue stars) for 1 sec. Participants were required to maintain the locations of these stars for a 3 sec delay period, utilizing their working memory. A probe object (a single green star of 1 sec duration) was then presented in either the same spot as one of the original test stars, or in a different spot than any of the original test stars. The participant was instructed to respond whether or not the probe star had the same or different location as one of the test stars. We implemented this task at the threshold perceptual span for each individual, which was defined by the number of test star objects that the individual could correctly encode without any working memory delay. For this, a brief perceptual thresholding period preceded the main working memory task, allowing for equivalent perceptual load to be investigated across participants[57]. During thresholding, the set size of test stars increased progressively from 1-8 stars based on accurate performance where 100% accuracy led to an increment in set size; **<**100% performance led to one 4-trial repeat of the same set size and any further inaccurate performance aborted the thresholding phase. The final set size at which 100% accuracy was obtained was designated as the individual's perceptual threshold. Post-thresholding, the working memory task consisted of 48 trials presented over 2 blocks[60]. The total task duration was 6 min.

5. Emotion Bias. Participants accessed a game-like assessment named *Face Off* adapted from studies of attentional bias in emotional contexts[61–63]. The task integrated a standardized set of culturally diverse faces from the NimStim database[64]. We used an equivalent number of male and female faces, each face with four sets of emotions, either neutral, positive (happy), negative (sad) or threatening (angry), presented on equivalent number of trials. Each task trial initiated with a central fixation "+" cue presented for 500 ms followed by an emotion face with a superimposed arrow of 300 ms duration. The arrow occurred in either the upper or lower central visual field on equal number of trials, and participants responded to the direction of the arrow (left/right) within an ensuing 1 sec response window. Participants completed 144 trials presented over three equipartitioned blocks with shuffled, but equivalent number of emotion trials in each block; a practice set of 4-trials preceded the main task. The total task duration was 10 min.

Electroencephalography (EEG). EEG data were collected simultaneous to the interoceptive attention assessment using a 24-channel Smarting^{TM} EEG amplifier with semi-dry and wireless electrodes in 10-20 standard layout. Data were acquired at 250 Hz sampling frequency at 24-bit resolution. Cognitive event markers were integrated using LSL and data files were stored in xdf format.

Behavioral Analyses. For the interoceptive attention task, behavioral data were analyzed for consistency of responses as participants made a response every two breaths. There were 31.0 ± 9.7 total responses across all subjects. Given that response times (RT) were not normally distributed within subjects,

performance consistency was calculated as 1 – (mad RT/ median RT), where mad is median absolute deviation of RT.

Behavioral performance on the external cognitive tasks of inhibitory control, interference processing, working memory, and emotion bias, was calculated as the efficiency metric for each task, which was then averaged to obtain global cognitive efficiency. Efficiency on each task was calculated as the product of task accuracy x speed[35,36]. Here, task accuracy was represented by the signal detection sensitivity, d', computed as z(Hits)-z(False Alarms)[65]; all d' values were divided by max theoretical d' of 4.65 to obtain scaled-d' in the 0-1 range. Cognitive task speeds were calculated as log(1/RT), where RT is response time in seconds. For the working memory task, thresholded perceptual span was also calculated for 1-8 items and normed in the 0-1 range, and working memory efficiency was weighted by span, i.e. span x accuracy x speed.

For all behavioral performance data, >3SD outlier data were removed prior to statistical analyses.

Interoceptive Attention Neural Analyses. We applied a uniform processing pipeline to all EEG data[30] acquired simultaneous to the interoceptive attention task. This included: 1) data pre-processing, 2) computing the EEG power spectrum, 3) cortical source localization of the EEG data to estimate source-level neural activity, and 4) functional connectivity across sources based on spectral amplitude time series correlations.

1) Data preprocessing was conducted using the EEGLAB toolbox in MATLAB[66]. EEG data was resampled at 250 Hz, and filtered in the 1-45 Hz range to exclude ultraslow DC drifts at <1Hz and high-frequency noise produced by muscle movements and external electrical sources at >45Hz. EEG data were average-referenced and epoched to the breath reports, i.e. LSL time-stamps for the finger-taps that participants made after every two breaths. Since the median response time across all subjects was 7.49 sec, we epoched response trials in the -3.7 sec to +3.7 sec response window. Any missing channel data were spherically interpolated to nearest neighbors. Epoched data were cleaned using the autorej function in EEGLAB to remove noisy trials (>5SD outliers rejected over max 8 iterations; 0.33 ± 0.12% of trials rejected per participant). EEG data were further cleaned by excluding signals estimated to be originating from non-brain sources, such as electrooculographic, electromyographic or unknown sources, using the Sparse Bayesian learning (SBL) algorithm (https://github.com/aojeda/PEB) explained below[67,68].

2) EEG power spectra were computed using the continuous wavelet transform (cwt) EEGLAB function across all channels and subjects and corresponding scalp topography of the average power spectrum was displayed using the topoplot EEGLAB function.

3) Cortical source localization was performed on the EEG data using the block-Sparse Bayesian learning (BSBL-2S) algorithm[67,68]. This is a two-step algorithm in which the first-step is equivalent to low-resolution electromagnetic tomography (LORETA[69]). LORETA estimates sources subject to smoothness constraints, i.e. nearby sources tend to be co-activated, which may produce source estimates with a high

number of false positives that are not biologically plausible. To guard against this, BSBL-2S applies sparsity constraints in the second step wherein blocks of irrelevant sources are pruned. This data-driven sparsity constraint of the BSBL-2S method reduces the effective number of sources considered at any given time as a solution, thereby reducing the ill-posed nature of the inverse mapping. In other words, one can either increase the number of channels used to solve the ill-posed inverse problem or impose more aggressive constraints on the solution to converge on the source model when channel density is low/moderate; 24 channels in this case. The BSBL-2S algorithm has been benchmarked to produce evidence-optimized inverse source models at 0.95AUC relative to the ground truth while without the second stage <0.9AUC is obtained[67,68]. Prior research also provides support that sparse source imaging constraints can be soundly applied to low channel density data[70,71], and we further shown that cortical source mapping with this method has high test-retest reliability[30]. Using BSBL-2s, we estimated source space activations and the root mean square signals were partitioned into cortical regions of interest (ROIs) and artifact sources. ROIs were based on the standard 68 brain region Desikan-Killiany atlas[38] using the Colin-27 head model[72]. Activations from artifact sources contributing to EEG noise from non-brain sources such as electrooculographic, electromyographic or unknown sources, were removed. Cleaned subject-wise data were then specifically filtered in theta (3-7 Hz), alpha (8-12 Hz), and beta (13-30 Hz) bands. In this research, we primarily focused on source localization of the alpha band signals, and secondarily also localized theta and beta band specific cortical ROI source signals. Filtered EEG data were then trial-averaged for high consistency trials (within 1 mad of median RT for each subject) and low-consistency trials (>1 mad of median RT for each subject). Across all subjects, there were 15.23 5.32 high consistency trials (50.99 1.06% of total trials) and 14.70 5.32 low consistency trials (49.01 1.06% of total trials). 1.74 3.82 trials (5.23 9.25% of total trials) were “faster” trials (i.e. had RTs < (median – 1 mad) RT) and were excluded from analyses given these types of trials were sparse. The source signal envelopes were computed in MATLAB (envelop function) by a spline interpolation over the local maxima separated by at least one time sample; we used this spectral amplitude signal for all neural analyses presented here. Specifically, we focused on the average spectral amplitude signal in the [-3.7 0] sec pre-response window as we were interested in the neural responses leading up to consistent versus inconsistent task performance. >5SD outlier removal was applied to all cortical source level activity prior to statistical analyses.

4) Functional connectivity was calculated between specific cortical sources of interest in the [-3.7 0] sec pre-response window using time-series Pearson correlations[73,74]. Correlation coefficients across participants were Fischer-z transformed to obtain normal distributions. Notably, source reconstruction prior to functional connectivity correlations, as we implement here, is one of the recommended strategies to alleviate the adverse effects of electric field spread/volume conductance across scalp EEG channels[75–77]. Source reconstruction unmixes the measured scalp signals to derive an estimate of the underlying sources and hence, minimizes the effect of volume conduction. While no strategy fully mitigates the effects of volume conduction, source correlations alleviate the problem similar to other strategies that capitalize on the out-of-phase interaction, discarding the interactions that are at a phase

difference of 0 (or 180°), such as calculations of the imaginary part of the coherency, the weighted phase lag index, or the phase slope index.

Statistical Analyses. We used robust linear regression, less sensitive to outliers than its non-robust version, to model interoceptive attention consistency based on demographic (age, sex, race, SES) and mental health trait (anxiety, depression, mindfulness) predictors. Robust linear regression models were also used to correlate interoceptive attention efficiency with global cognitive efficiency averaged across the four external cognitive tasks, and to correlate consistency with efficiency on each cognitive task. Significant model results were reported with confidence intervals.

We conducted our primary neural source analyses in the alpha band as this was the dominant frequency in eyes-closed state. Alpha activity in the pre-response time window on high vs. low consistency trials was compared within-subjects using paired t-tests. We applied fwer-corrections for multiple comparisons across all 68 ROIs. These analyses were secondarily conducted in the theta and beta bands and correlated with the results in the alpha band for comparison across frequency bands. We then focused on specific DMN and cognitive control ROIs, i.e. Precuneus, DLPFC, Insula and ACC. Medial ROIs, i.e. Precuneus and ACC were left/right averaged, while for lateral ROIs, i.e. DLPFC and Insula we focused on the left hemisphere given its role in positive affect representation[25,29,30,39–41]. Functional connectivity across these specific ROIs were also compared using paired t-tests with fwer-corrections applied for multiple comparisons. Estimation plots for changes across high vs. low consistency trials were generated using the MATLAB DABEST toolbox (https://github.com/ACCLAB/DABEST-Matlab).

Finally, we generated multiple regression models for mindfulness based on DMN and cognitive control region selective activity or functional connectivity predictors; anxiety and depression covariates were accounted for in these models.

References

1. Luna, B., Marek, S., Larsen, B., Tervo-Clemmens, B. & Chahal, R. An Integrative Model of the Maturation of Cognitive Control. *Annu. Rev. Neurosci.* **38**, 151–170 (2015).

2. Badre, D. Defining an Ontology of Cognitive Control Requires Attention to Component Interactions. *Top. Cogn. Sci.* **3**, 217–221 (2011).

3. Mishra, J., Anguera, J. A., Ziegler, D. A. & Gazzaley, A. *A cognitive framework for understanding and improving interference resolution in the brain*. *Progress in Brain Research* vol. 207 (2013).

4. Dosenbach, N. U. F. *et al.* A Core System for the Implementation of Task Sets. *Neuron* **50**, 799–812 (2006).

5. Menon, V. & Uddin, L. Q. Saliency, switching, attention and control: a network model of insula function. *Brain Struct. Funct.* **214**, 655–67 (2010).

6. Buckner, R. L., Andrews-Hanna, J. R. & Schacter, D. L. The brain's default network: anatomy, function, and relevance to disease. *Ann. N. Y. Acad. Sci.* **1124**, 1–38 (2008).

7. Mason, M. F. *et al.* Wandering minds: the default network and stimulus-independent thought. *Science* **315**, 393–5 (2007).

8. Christoff, K., Irving, Z. C., Fox, K. C. R., Spreng, R. N. & Andrews-Hanna, J. R. Mind-wandering as spontaneous thought: a dynamic framework. *Nat. Rev. Neurosci. 2016 1711* **17**, 718–731 (2016).

9. Chun, M. M., Golomb, J. D. & Turk-Browne, N. B. A Taxonomy of External and Internal Attention. *Annu. Rev. Psychol.* **62**, 73–101 (2011).

10. Maric, V., Ramanathan, D. & Mishra, J. Respiratory regulation & interactions with neuro-cognitive circuitry. *Neurosci. Biobehav. Rev.* **112**, 95–106 (2020).

11. Lutz, A., Slagter, H. A., Dunne, J. D. & Davidson, R. J. Attention regulation and monitoring in meditation. *Trends Cogn. Sci.* **12**, 163–169 (2008).

12. Davidson, R. J. Mindfulness-Based Cognitive Therapy and the Prevention of Depressive Relapse: Measures, Mechanisms, and Mediators. *JAMA Psychiatry* **73**, 547–548 (2016).

13. Deng, Y.-Q., Li, S. & Tang, Y.-Y. The Relationship Between Wandering Mind, Depression and Mindfulness. *Mindfulness (N. Y).* **5**, 124–128 (2014).

14. Levinson, D. B., Stoll, E. L., Kindy, S. D., Merry, H. L. & Davidson, R. J. A mind you can count on: validating breath counting as a behavioral measure of mindfulness. *Front. Psychol.* **5**, (2014).

15. Brefczynski-Lewis, J. A., Lutz, A., Schaefer, H. S., Levinson, D. B. & Davidson, R. J. Neural correlates of attentional expertise in long-term meditation practitioners. *Proc. Natl. Acad. Sci. U. S. A.* **104**, 11483–8 (2007).

16. Brewer, J. A. *et al.* Meditation experience is associated with differences in default mode network activity and connectivity. *Proc. Natl. Acad. Sci. U. S. A.* **108**, 20254–20259 (2011).

17. Dickenson, J., Berkman, E. T., Arch, J. & Lieberman, M. D. Neural correlates of focused attention during a brief mindfulness induction. *Soc. Cogn. Affect. Neurosci.* **8**, 40–47 (2013).

18. Farb, N. *et al.* Interoception, contemplative practice, and health. *Front. Psychol.* **0**, 763 (2015).

19. Hölzel, B. K. *et al.* Differential engagement of anterior cingulate and adjacent medial frontal cortex in adept meditators and non-meditators. *Neurosci. Lett.* **421**, 16–21 (2007).

20. Hasenkamp, W., Wilson-Mendenhall, C. D., Duncan, E. & Barsalou, L. W. Mind wandering and attention during focused meditation: A fine-grained temporal analysis of fluctuating cognitive states. *Neuroimage* **59**, 750–760 (2012).

21. Bauer, C. C. C., Whitfield-Gabrieli, S., Díaz, J. L., Pasaye, E. H. & Barrios, F. A. From state-to-trait meditation: Reconfiguration of central executive and default mode networks. *eNeuro* **6**, (2019).

22. Scheibner, H. J., Bogler, C., Gleich, T., Haynes, J. D. & Bermpohl, F. Internal and external attention and the default mode network. *Neuroimage* **148**, 381–389 (2017).

23. Garrison, K. A., Zeffiro, T. A., Scheinost, D., Constable, R. T. & Brewer, J. A. Meditation leads to reduced default mode network activity beyond an active task. *Cogn. Affect. Behav. Neurosci.* **15**, 712–720 (2015).

24. Mishra, J. *et al.* Closed-loop digital meditation for neurocognitive and behavioral development in adolescents with childhood neglect. *Transl. Psychiatry* **10**, 1–13 (2020).

25. Tang, Y.-Y., Hölzel, B. K. & Posner, M. I. The neuroscience of mindfulness meditation. *Nat. Rev. Neurosci.* **16**, 213–225 (2015).

26. Voss, M. J., Zukosky, M. & Wang, R. F. A new approach to differentiate states of mind wandering: Effects of working memory capacity. *Cognition* **179**, 202–212 (2018).

27. Nyklíček, I. Aspects of Self-Awareness in Meditators and Meditation-Naïve Participants: Self-Report Versus Task Performance. *Mindfulness 2020 114* **11**, 1028–1037 (2020).

28. Boudreau, B. & Poulin, C. An examination of the validity of the Family Affluence Scale II (FAS II) in a general adolescent population of Canada. *Soc. Indic. Res.* **94**, 29–42 (2009).

29. Grennan, G. *et al.* Cognitive and Neural Correlates of Loneliness and Wisdom during Emotional Bias. *Cereb. Cortex* (2021) doi:10.1093/cercor/bhab012.

30. Balasubramani, P. P. *et al.* Mapping cognitive brain functions at scale. *Neuroimage* **231**, 117641 (2021).

31. Spitzer, R. L., Kroenke, K., Williams, J. B. W. & Loewe, B. A Brief Measure for Assessing Generalized Anxiety Disorder: The GAD-7. *Arch. Intern. Med.* **166**, 1092–1097 (2006).

32. Kroenke, K., Spitzer, R. L. & Williams, J. B. W. The PHQ-9. Validity of a Brief Depression Severity Measure. *J. Gen. Intern. Med.* **16**, 606–613 (2001).

33. Brown, K. W. & Ryan, R. M. The Benefits of Being Present: Mindfulness and Its Role in Psychological Well-Being. *J. Pers. Soc. Psychol.* **84**, 822–848 (2003).

34. Shah, R. V. *et al.* Personalized machine learning of depressed mood using wearables. *Transl. Psychiatry* **11**, 338 (2021).

35. Barlow, H. B. The absolute efficiency of perceptual decisions. *Philos. Trans. R. Soc. Lond. B. Biol. Sci.* **290**, 71–82 (1980).

36. Vandierendonck, A. A comparison of methods to combine speed and accuracy measures of performance: A rejoinder on the binning procedure. *Behav. Res. Methods* **49**, 653–673 (2017).

37. Clayton, M. S., Yeung, N. & Kadosh, R. C. The many characters of visual alpha oscillations. *Eur. J. Neurosci.* **48**, 2498–2508 (2018).

38. Desikan, R. S. *et al.* An automated labeling system for subdividing the human cerebral cortex on MRI scans into gyral based regions of interest. *Neuroimage* **31**, 968–80 (2006).

39. Allen, J. J. B. & Kline, J. P. Frontal EEG asymmetry, emotion, and psychopathology: the first, and the next 25 years. *Biol. Psychol.* **67**, 1–5 (2004).

40. Cacioppo, J. T. Feelings and emotions: roles for electrophysiological markers. *Biol. Psychol.* **67**, 235–243 (2004).

41. Davidson, R. J. *et al.* Alterations in Brain and Immune Function Produced by Mindfulness Meditation. *Psychosom Med* **65**, 564–570 (2003).

42. Kucyi, A., Esterman, M., Riley, C. S. & Valera, E. M. Spontaneous default network activity reflects behavioral variability independent of mind-wandering. *Proc. Natl. Acad. Sci.* **113**, 13899–13904 (2016).

43. Esterman, M., Noonan, S. K., Rosenberg, M. & DeGutis, J. In the Zone or Zoning Out? Tracking Behavioral and Neural Fluctuations During Sustained Attention. *Cereb. Cortex* **23**, 2712–2723 (2012).

44. Kucyi, A., Hove, M., Esterman, M., Hutchison, R. & Valera, E. Dynamic Brain Network Correlates of Spontaneous Fluctuations in Attention. *Cereb. Cortex* **27**, 1831–1840 (2017).

45. Carr, L., Iacoboni, M., Dubeau, M.-C., Mazziotta, J. C. & Lenzi, G. L. Neural mechanisms of empathy in humans: a relay from neural systems for imitation to limbic areas. *Proc. Natl. Acad. Sci. U. S. A.* **100**, 5497–5502 (2003).

46. Goldin, P. R., McRae, K., Ramel, W. & Gross, J. J. The Neural Bases of Emotion Regulation: Reappraisal and Suppression of Negative Emotion. *Biol. Psychiatry* **63**, 577–586 (2008).

47. Posner, M. I. & Rothbart, M. K. Toward a physical basis of attention and self regulation. *Phys. Life Rev.* **6**, 103–20 (2009).

48. Ziegler, D. A. *et al.* Closed-loop digital meditation improves sustained attention in young adults. *Nat. Hum. Behav.* **3**, 746–757 (2019).

49. Klimecki, O. M., Leiberg, S., Lamm, C. & Singer, T. Functional neural plasticity and associated changes in positive affect after compassion training. *Cereb. Cortex* **23**, 1552–1561 (2013).

50. Spitzer, R. L., Kroenke, K., Williams, J. B. W. & Löwe, B. A Brief Measure for Assessing Generalized Anxiety Disorder: The GAD-7. *Arch. Intern. Med.* **166**, 1092–1097 (2006).

51. De Bruin, E. I., Zijlstra, B. J. H., Van De Weijer-Bergsma, E. & Boegels, S. M. The Mindful Attention Awareness Scale for Adolescents (MAAS-A): Psychometric Properties in a Dutch Sample. *Mindfulness (N. Y).* **2**, 201–211 (2011).

52. Misra, A., Ojeda, A. & Mishra, J. BrainE: a digital platform for evaluating, engaging and enhancing brain function. Regents of the University of California Copyright SD2018-816. (2018).

53. Kothe, C., Medine, D., Boulay, C., Grivich, M. & Stenner, T. 'Lab Streaming Layer' Copyright. https://labstreaminglayer.readthedocs.io/ (2019).

54. Greenberg, L. M. & Waldman, I. D. Developmental normative data on the test of variables of attention (T.O.V.A.). *J. Child Psychol. Psychiatry.* **34**, 1019–30 (1993).

55. Fakhraei, L. *et al.* Mapping large-scale networks associated with action, behavioral inhibition and impulsivity. *eNeuro* **8**, 1–20 (2021).

56. Eriksen, B. A. & Eriksen, C. W. Effects of noise letters upon identification of a target letter in a non-search task. *Percept. Psychophys.* **16**, 143–149 (1974).

57. Lavie, N., Hirst, A., de Fockert, J. W. & Viding, E. Load Theory of Selective Attention and Cognitive Control. *J. Exp. Psychol. Gen.* **133**, 339–354 (2004).

58. Shipstead, Z., Harrison, T. L. & Engle, R. W. Working memory capacity and visual attention: Top-down and bottom-up guidance. *Q. J. Exp. Psychol.* **65**, 401–407 (2012).

59. Sternberg, S. High-speed scanning in human memory. *Science (80-.).* **153**, 652–654 (1966).

60. Lenartowicz, A. *et al.* Electroencephalography Correlates of Spatial Working Memory Deficits in Attention-Deficit/Hyperactivity Disorder: Vigilance, Encoding, and Maintenance. *J. Neurosci.* **34**, 1171–1182 (2014).

61. Grennan, G. *et al.* Cognitive and Neural Correlates of Loneliness and Wisdom during Emotional Bias. *Cereb. Cortex* **31**, 3311–3322 (2021).

62. López-Martín, S., Albert, J., Fernández-Jaén, A. & Carretié, L. Emotional distraction in boys with ADHD: Neural and behavioral correlates. *Brain Cogn.* **83**, 10–20 (2013).

63. López-Martín, S., Albert, J., Fernández-Jaén, A. & Carretié, L. Emotional response inhibition in children with attention-deficit/hyperactivity disorder: neural and behavioural data. *Psychol. Med.* **45**,

2057–2071 (2015).

64. Tottenham, N. *et al.* The NimStim set of facial expressions: Judgments from untrained research participants. *Psychiatry Res.* **168**, 242–249 (2009).

65. Heeger, D. & Landy, M. Signal detection theory. in *Encyclopedia of perception* (ed. Goldstein, B.) 887–892 (SAGE Publications, 2009).

66. Delorme, A. & Makeig, S. EEGLAB: an open source toolbox for analysis of single-trial EEG dynamics including independent component analysis. *J. Neurosci. Methods* **134**, 9–21 (2004).

67. Ojeda, A., Kreutz-Delgado, K. & Mullen, T. Fast and robust Block-Sparse Bayesian learning for EEG source imaging. *Neuroimage* **174**, 449–462 (2018).

68. Ojeda, A., Kreutz-Delgado, K. & Mishra, J. Bridging M/EEG Source Imaging and Independent Component Analysis Frameworks Using Biologically Inspired Sparsity Priors. *Neural Comput.* **33**, 1–31 (2021).

69. Pascual-Marqui, R. D., Michel, C. M. & Lehmann, D. Low resolution electromagnetic tomography: a new method for localizing electrical activity in the brain. *Int. J. Psychophysiol.* **18**, 49–65 (1994).

70. Ding, L. & He, B. Sparse source imaging in electroencephalography with accurate field modeling. *Hum. Brain Mapp.* **29**, 1053 (2008).

71. Stopczynski, A. *et al.* Smartphones as pocketable labs: Visions for mobile brain imaging and neurofeedback. *Int. J. Psychophysiol.* **91**, 54–66 (2013).

72. Holmes, C. J. *et al.* Enhancement of MR images using registration for signal averaging. *J. Comput. Assist. Tomogr.* **22**, 324–333 (1998).

73. Coquelet, N. *et al.* Comparing MEG and high-density EEG for intrinsic functional connectivity mapping. *Neuroimage* **210**, 116556 (2020).

74. Hlinka, J., Alexakis, C., Diukova, A., Liddle, P. F. & Auer, D. P. Slow EEG pattern predicts reduced intrinsic functional connectivity in the default mode network: An inter-subject analysis. *Neuroimage* **53**, 239–246 (2010).

75. Mishra, J. *et al.* Closed-loop Neurofeedback of Alpha Synchrony during Goal-directed Attention. *J. Neurosci.* JN-RM-3235-20 (2021) doi:10.1523/JNEUROSCI.3235-20.2021.

76. Schoffelen, J. M. & Gross, J. Source connectivity analysis with MEG and EEG. *Human Brain Mapping* vol. 30 1857–1865 (2009).

77. Bastos, A. M. & Schoffelen, J. M. A tutorial review of functional connectivity analysis methods and their interpretational pitfalls. *Frontiers in Systems Neuroscience* vol. 9 (2016).

Figures

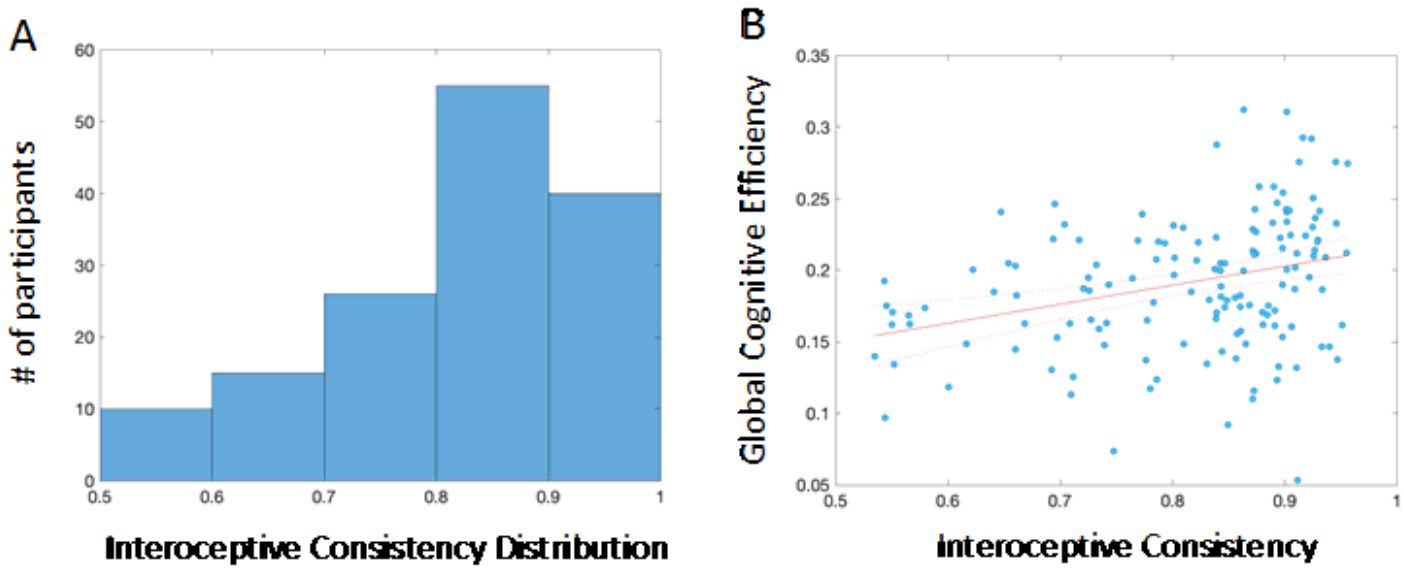

Figure 1

Interoceptive attention to breathing evaluated using the consistency of performance metric. The task simply instructed participants to close their eyes and tap after every two breaths with a blank screen shown during task. (A) Distribution of interoceptive attention consistency was calculated based on breath monitoring responses across 161 subjects. (B) Significant robust regression of interoceptive consistency was found with global cognitive efficiency averaged across the cognitive domains of inhibitory control, working memory, interference processing and emotion bias ($\beta = 0.133 \pm 0.034$, $p = 0.0001$).

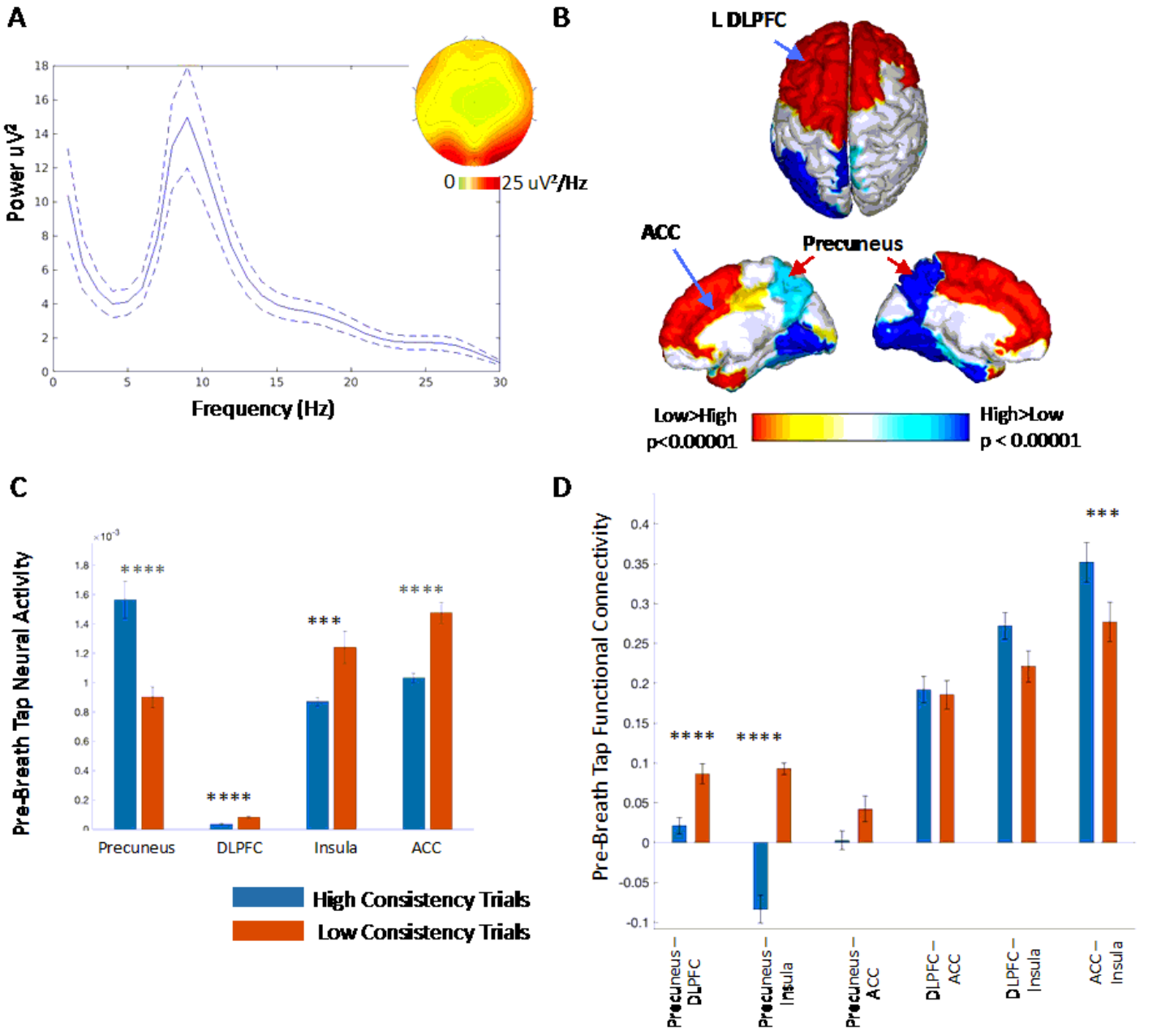

Figure 2

Spectro-temporal activity during eyes closed interoceptive attention to breathing. A) The EEG power spectrum on the eyes-closed task shows alpha dominance; spectral data are averaged across all electrodes and subjects, and dashed lines represent 95%le confidence intervals. Inset shows the alpha band (8-12 Hz) scalp topography. (B) Significant differences in cortical source localized alpha band activity prior to breath reporting are shown contrasting high vs. low consistency performance trials; high consistency trials were those with response times (RTs) within 1 mad of the median RT for each subject while low consistency trials had RTs > 1 mad RT. (C) Alpha activity in select regions of interest for the DMN Precuneus versus cognitive control regions of the left DLPFC and cingulo-opercular network regions (medial ACC, left Insula) are shown with opposing activations observed on high versus low consistency interoceptive attention trials. (D) Functional connectivity relationships between DMN and cognitive

control regions were significant for Precuneus – DLPFC and Precuneus – Insula with greater connectivity on low consistency trials, while ACC – Insula connectivity showed the opposite result. All results are fwer-corrected for multiple comparisons. *** p<.001 or **** p<.0001

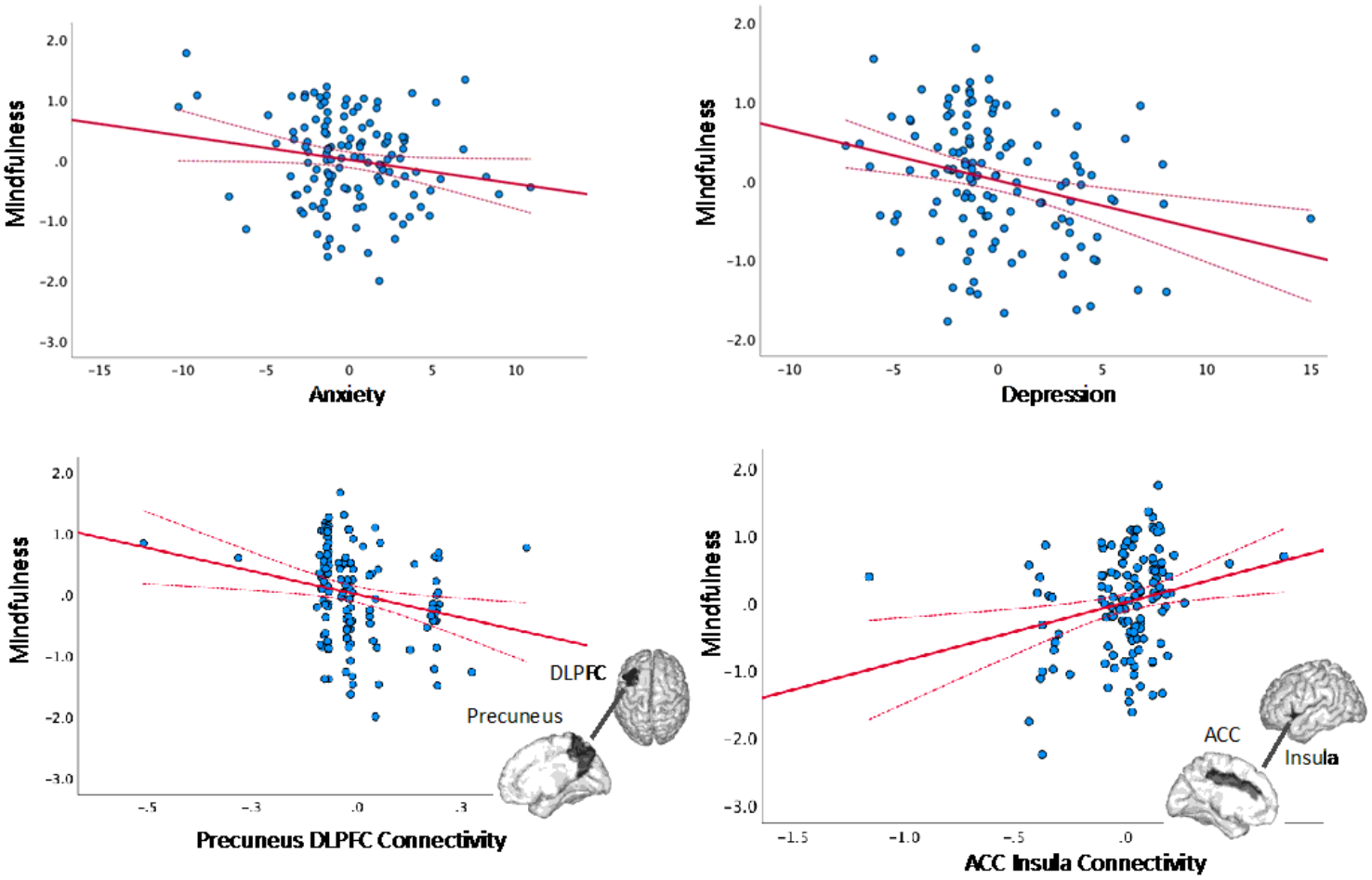

Figure 3

Partial regression plots for the significant predictors of mindfulness include anxiety, depression (top) and Precuneus – DLPFC and ACC – Insula functional connectivity (bottom). The functional connections are calculated as the difference in connectivity on high versus low consistency trials; Precuneus – DLPFC connectivity is a negative predictor while ACC - Insula connectivity is a positive predictor of mindfulness.

Supplementary Files

This is a list of supplementary files associated with this preprint. Click to download.

- SupplementaryFigures.docx